Comprehensive analysis of the landscape characteristics of m6A regulators in acute myeloid leukemia

Xinai Liao
Fujian Medical University Union Hospital
Ling Chen
Fujian Medical University Union Hospital
Jingru Liu
Fujian Medical University Union Hospital
Haoran Hu
Fujian Medical University Union Hospital
Diyu Hou
Fujian Medical University Union Hospital
Ruolan You
Fujian Medical University Union Hospital
Xiaoting Wang
Fujian Medical University Union Hospital
Huifang Huang (huanghuif@fjmu.edu.cn)
Fujian Medical University Union Hospital https://orcid.org/0000-0003-2691-1147

Research Article

Keywords: AML, m6A, m6A regulators, prognostic, tumor microenvironment

Posted Date: April 12th, 2022

DOI: https://doi.org/10.21203/rs.3.rs-1511744/v1

Abstract

Background: Patients with acute myeloid leukemia (AML) have a poor prognosis and low overall survival (OS) rate owing to its heterogeneity and the complexity of its tumor microenvironment (TME). N6-methyladenosine (m^6A) modification plays a potential role in the initiation and progression of haematopoietic malignancies. Nonetheless, compressive analysis of RNA m^6A modification is rare in AML.

Methods: Based on somatic mutation and copy number analysis, differential expression analysis, survival analysis, function enrichment analysis, spearman correlation analysis, gene set enrichment analyses and a series of experiments (western blot, quantitative reverse transcription polymerase chain reaction and flow cytometry), data from The Cancer Genome Atlas (TCGA) and Gene Expression Omnibus (GEO) database were used to assess the value of m^6A regulators in the development and prognosis of AML.

Results: Compared with normal samples, five m^6A regulators were significantly differentially expressed in AML samples. Among them, methyltransferase-like 14 (METTL14), zinc finger CCCH-type containing 13 (ZC3H13), RNA binding motif protein 15 (RBM15) and YTH domain-containing 2 (YTHDC2) were associated with the OS of AML patients. Notably, they were successfully validated in clinical samples. Besides, three distinct m^6A modification patterns were determined, and remarkable differences were observed in the expression of m^6A regulators, TME infiltration characterization, functional enrichment and survival outcome among these patterns. We further found 122 m^6A phenotype-related differentially expressed genes (DEGs). Functional enrichment analysis revealed that the DEGs were closely relevant to metabolism. Based on 28 prognosis-related DEGs, m6Ascore system was established to evaluate patient prognosis, patients with high m6Ascore had higher survival rates than those with low m6Ascore. Importantly, m6Ascore may serve as a potential predictor independent of TMB.

Conclusion: This work provided new insight into the potential functions of m^6A regulators in the initiation and progression of AML. It indicated that some m^6A regulators may serve novel biomarkers to predict the prognosis of AML.

1. Introduction

Acute myeloid leukemia (AML) is a life-threatening haematological malignancy and is associated with poor prognosis and low overall survival (OS) [1]. In a study, 19,940 new cases of AML and 11,180 AML-related deaths were projected to occur in the United States of America in 2020 [2]. With the emergence of various therapies, remarkable remission can be initially attained in most AML patients; however, complete remission is rare [3]. Therefore, identifying potential biomarkers of AML may help in improving treatment strategies and assessing prognosis.

Several factors such as genetics, proteomics and epigenetic processes were associated with cell differentiation and haematopoiesis in AML [4]. In addition to DNA methylation and histone modification, RNA modification has been identified as a common phenomenon and a key regulator of RNA transcription and stability in various types of diseases since the identification of RNA demethylases[5, 6]. N6-methyladenosine (m^6A) is considered the most major methylation in eukaryotic mRNAs. Its reversible methylation significantly affects gene expression regulation [7, 8]. m^6A methylation and expression levels of its regulators are frequently dysregulated in tumors [9, 10], neurological diseases [11, 12] and embryonic retardation [13]. A growing number of studies regarding the role of m^6A regulators in AML such as fat mass and obesity-associated protein (FTO) [14], methyltransferase-like 3 / methyltransferase-like 14 [15], and YTH N6-methyladenosine RNA binding protein 2 (YTHDF2) [16]. However, many researches only considered one or several m^6A regulators, and there have few systematic research into it. The potential role of RNA m^6A modification in AML remains unclear.

In the current study, we aimed to conduct a comprehensive investigation of the landscape characteristics of m^6A regulators in AML. The genomic information of AML patients and normal individuals were obtained from the Cancer Genome Atlas (TCGA) and Gene Expression Omnibus (GEO). We systematically evaluated the genetic variation and differential expression of m^6A regulators in AML. And screened for the key m^6A regulators related to OS, thus providing possible prognostic markers for AML. In addition, we constructed three distinct m^6A modification patterns, and there were obvious differences in pathway enrichment and TME cell infiltration characteristics. Subsequently established m6Ascore to explore its value in predicting AML prognosis. Briefly, the results may contribute to better understand the role of m^6A regulators and lead to improved prognosis in AML.

2. Materials And Methods

2.1 Isolation of peripheral blood mononuclear cells (PBMCs)

The samples of human were collected from patients with newly diagnosed AML and healthy donors at Fujian Medical University Union Hospital, Fuzhou, China. Details on AML patient samples are shown in Table 1. The study was approved by the Committee for the Ethical Review of Research, Fujian Medical University Union Hospital and informed consent was obtained from all the patients. PBMCs were isolated through Ficoll gradient.

2.2 Processing of RNA-seq-based data

The RNA-seq-based data and clinical information of 151 AML samples were downloaded from TCGA database (https://portal.gdc.cancer.gov/) using the R package TCGAbiolinks [17], which was specifically developed for integrative analysis of GDC data. Subsequently, RNA-seq data (FPKM values) were then converted to transcripts per kilobase million (TPM) values using the limma package [18]. Normalised

array data [GSE9476 (38 normal and 26 AML samples), GPL96 (HG-U133A) Affymetrix Human Genome U133A Array] and GSE23312 [GPL10107 (SMD Print_1094 Homo sapiens)] were obtained from the Gene Expression Omnibus (GEO) database. Gene expression profile matrix files of GSE9476 and GSE2331 were obtained from raw datasets using Perl [19]. Somatic mutation data were downloaded from TCGA database, and the copy number of all AML genes was obtained from the UCSC dataset.

2.3 Somatic mutation and copy number analysis of m^{6}A regulators

To analyse the mutations and copy number variations (CNVs) of m^{6}A regulators in AML samples, somatic mutation data were obtained from TCGA database and analysed using Perl and the R package maptools [20]. The copy number of m^{6}A regulators was evaluated using the R packages (version 4.1.1) and Perl. The differential expression of m^{6}A regulators in normal and AML samples were analysed using the R software. The Pearson correlation algorithm was used to analyse the correlation of m^{6}A regulators with the occurrence and development of AML.

2.4 Unsupervised clustering of 22 m^{6}A regulators

Only a few m^{6}A regulators were detected using the Illumina HumanRef-8 WG-DASL v3.0 platform, 22 regulators were acquired from TCGA and GSE9476 datasets to identify different m^{6}A modification patterns mediated by m^{6}A regulators, including 8 writers (METTL3, METTL14, METTL16, WTAP, VIRMA, ZC3H13, RBM15 and RBM15B), 1 eraser (FTO) and 13 readers (YTHDC1, YTHDC2, YTHDF1, YTHDF2, YTHDF3, HNRNPC, FMR1, LRPPRC, HNRNPA2B1, IGFBP1, IGFBP2, IGFBP3 and RBMX). The established unsupervised clustering was used to determine different m^{6}A modification patterns according to the expression of the 22 m^{6}A regulators and classify patients for further analysis. The ConsensusClusterPlus and limma packages were used to perform the abovementioned analyses, which were repeated 1000 times to ensure the stability of the classification [21]. Subsequently, the differential expression of m^{6}A regulators in different phenotypes were analysed using the limma [18], reshape2 and Nagpur packages [22].

2.5 Gene set variation analysis (GSVA) of the m^{6}A regulators

Gene set variation analysis (GSVA), which is a nonparametric and unsupervised method usually used to estimate changes in pathways and biological processes [23].We used R package ‘GSVA’ to analyse differences enrichments in biological processes between m^{6}A modification patterns. The gene set ‘C2. Cp.kegg. V6.2. Symbols was downloaded from MSigDB for GSVA. A *P*-value < 0.05 was considered statistically significant.

2.6 Survival analysis of m^{6}A regulators in patients with AML

To predict the prognostic value of m^{6}A regulators, survival analysis was performed using clinical data obtained from TCGA. And we verified some key genes in the GEO database. Kaplan–Meier (KM) survival curves of m^{6}A regulators were plotted using the survival and survminer packages [24], and differences in survival rate were assessed using a log-rank test threshold of *P*-value < 0.05.

2.7 Identification of differentially expressed genes (DEGs) among distinct m^{6}A phenotypes

The limma package was used to screen for m^{6}A phenotype-related DEGs among the three m^{6}A modification patterns identified from the abovementioned analyses [18], with a threshold of adjusted *P*-value < 0.001

2.8 Pathway and Gene Ontology enrichment

After obtaining the Entrez-ID of each DEG using the 'org.Hs.eg.db' R package, Gene Ontology (GO) and Kyoto Encyclopedia of Genes and Genomes (KEGG) pathway analyses of these DEGs were performed using the 'clusterProfiler' packages [25]. GO analysis can be divided into three categories as follows: biological processes (BPs), cellular components (CCs) and molecular functions (MFs). A *P*-value < 0.05 was considered significant for the Fisher's exact test.

2.9 Tumor mutational burden (TMB) estimation and prognostic analysis

A scoring system was constructed to evaluate the m^{6}A modification patterns of patients with AML-m^{6}A regulator features, which was called m6Ascore. First, we screened for DEGs related to prognosis using a univariate Cox regression, and genes significantly related to prognosis were extracted for further analysis. Subsequently, principal component analysis (PCA) was performed to construct m^{6}A regulators features. Finally, we defined the m6Ascore using a method similar to GGI [26], which is as follows:

$$\text{m6Ascore} = \sum(\text{PC1i} + \text{PC2i})$$

In this equation, i represents the expression of m^{6}A phenotype-related genes.

Patients were divided into the high- and low-m6A-score groups based on the median score, and survival analysis was performed based on m6Ascores using the survival package. We extracted the somatic mutation data using Perl and estimated TMB values by dividing the number of somatic mutations by the total length of exons. Additionally, we performed KM survival analysis to compare OS between TMB subgroups and examined the relationship between TMB and m6Ascores via correlation analysis.

2.10 Evaluation of TME cell infiltration

Single-sample gene set enrichment analysis (ssGSEA) was used to quantify the relative abundance of infiltrating immune cells in the TME of AML using the ssGSEA package. The gene set used to label each infiltrating immune cell type of TME was obtained from a study by Charoentong [27, 28]. The gene set

contains data regarding various human immune cell subtypes, including activated B cells, activated dendritic cells, T follicular helper cells, eosinophils and regulatory T cells. The enrichment fraction calculated using ssGSEA was used to represent the relative abundance of infiltrating immune cells in each sample. The Pearson correlation algorithm was used to analyse the correlation between m^6A regulators and m6Ascore.

2.11 Quantitative reverse transcription polymerase chain reaction (qRT-PCR)

The TRIzol reagent (Invitrogen) was used to extract total RNA from PBMCs. cDNA was synthesised using 5×All-in-One RT MasterMix with AccuRT (abm, Canada), and Eva Green 2×qPCR MasterMix-Low ROX (abm, Canada) was used to evaluate mRNA levels. The primer sequences are listed in Table S1.

2.12 Western blot

Total proteins from PBMCs were extracted by RIPA buffer (Beyotime) containing protease and phosphatase inhibitor cocktail (Thermo). And concentration was determined using a BCA Protein Assay Kit (Thermo). Proteins were separated using SDS-PAGE (10% gels) and transferred onto polyvinylidene difluoride (PVDF) membranes. Subsequently, the membranes were blocked with 5% BSA at room temperature for 1 h and incubated with primary antibodies overnight at 4°C. The following day, the membranes were incubated with HRP-conjugated secondary antibodies (Beyotime, #A0208, #A0216) at room temperature for 1 h. Chemiluminescence signals were visualised with a BeyoECL Star Kit (Beyotime).

2.13 Flow cytometry

All FCM studies were performed using single cell suspensions, and cells were stained in accordance with the standard protocols. Antibodies recognising CD45-eFluor506 (#69045942, Thermo), CD4-Percp/Cyanine5.5 (#30050, Biolegend), CD8-Bv786 (#563823, BD Pharmingen,), CD3-FITC, CD16/CD56-PE (#A07735, Beckman) and CD19-PerCP5 (#302227, Biolegend) were used. Samples were analyzed using a flow cytometer (BD Biosciences) and subsequent analysis was performed using FlowJo 10.1 software.

2.14 Statistical analysis

All experiments were performed in triplicate. The GraphPad Prism (version 9.2, GraphPad Software, La Jolla, CA, USA) was used for statistical analysis of all experimental data. Data were presented as mean ± SDs. The student's t-test was performed for between-group comparisons. A P-value < 0.05 was considered statistically significant.

3. Results

3.1 Genetic variation landscape of m^6A regulators in AML

In this study, there were 22 m^6A regulators, including 8 writers, 1 eraser and 13 readers were identified. First, we evaluated the CNVs and somatic mutations of 22 m^6A regulators in patients with AML. Among the 143 samples, only 19 had mutations of m^6A regulators, with a frequency of 13.29%, and METLL14, WTAP, ZC3H13 and YTHDC2 exhibited the highest mutation frequency, followed by RBM15, FMR1 and LRPPRC (Fig. 1A). In addition, we found that most m^6A regulators had copy number deletions, whereas YTHDF1, YTHDF2, YTHDF3 and FTO had copy number gain (Fig. 1B). Figure 1C shows the location of CNVs of m^6A regulators on chromosomes. Correlation analysis discovered that there was closely coordination among m^6A regulators (Fig. 1D). We then examined the mRNA expression levels of the m^6A regulators and observed that AML patients exhibited increases in the expression of ZC3H13, RBM15 and LRPPRC, whereas presented decreases in METTL14 and YTHDC2 (Fig. 1E). The above results indicated that the mutation and CNV alterations of m^6A regulators could influence their expression in AML. We also noted that an imbalance in the expression of m^6A regulators might play a crucial role in the occurrence and progression of AML.

3.2 Overall survival analysis of m^6A regulators

To determine the potential role of m^6A regulators in predicting the OS of AML patients, we constructed KM survival curves. Based on TCGA data, a total of 11 genes were verified to be significantly associated with AML prognosis. As shown in Fig. 2, ZCH13H ($P = 0.043$), YTHDF1 ($P = 0.023$), RBM15 ($P = 0.014$), METLL3 ($P = 0.003$) and HNRNPC ($P = 0.005$) were related to poor OS, whereas YTHDC2 ($P = 0.043$), FTO ($P < 0.001$), METTL14 ($P = 0.018$), YTHDF3 ($P = 0.05$), IGFBP3 ($P = 0.02$) and IGFBP2 ($P = 0.011$) were significantly associated with increased OS. In addition, the results of univariate Cox regression also demonstrated that METTL3, YTHDF1, RBM15, ZC3H13 and HNRNPC were significantly correlated with poor OS (Figure S1).

3.3 Characteristics of AML somatic mutation and correlation of m^6A regulators with TP53

Somatic mutation analysis demonstrated that DNMT3A (13%), FLT3 (11%), NPM1 (9%), RUNX1 (9%), IDH2 (8%), MUC16 (8%), TP53 (8%), TTN (8%), KIT (6%) and NRAS (6%) were the top 10 mutant genes (Fig. 3A). Further investigation revealed that missense mutations, SNPs and C > T alterations were responsible for a wide variety of classification groups. When each sample was evaluated separately, there presented a median of 10 mutations and a maximum of 1355 mutations. Besides, the top 10 genes differed from the previous ones when multiple hits were counted independently and the overall number of mutations was considered (Fig. 3B). TP53 is known to play an important role in AML development. To better understand the association between m^6A regulators and TP53 expression in AML. We next applied correlation analysis and observed that TP53 expression was positively correlated to METTL14, RBM15, IGFBP1, WTAP and YTHDC2, and was negatively relevant to other m6A regulators (Fig. 3C). The above suggested that m^6A regulators may act a significant role in regulating the expression of TP53 thereby promote the progression of AML.

3.4 Patterns of m^{6}A methylation modification and its biological characteristics in AML

Based on the expression of 22 m^{6}A regulators, we used the ConsensusClusterPlus R package to classify patients with qualitatively different m^{6}A modification patterns. As the stability of k-means clustering increased from 2 to 9 in TCGA datasets, k = 3 was considered an acceptable value. The identified patterns were named m6Acluster-A, m6Acluster-B and m6Acluster-C. (Fig. 4A–B). The results of PCA revealed evident differences among the three subgroups (Figure S2A). We compared the clinicopathological characteristics of these three subgroups and the discrepancy seemed not obviously. (Figure S2B). To further investigate the characteristics of these m^{6}A modification phenotypes in biological behaviours, we performed GSVA enrichment analysis. We found that m6Acluster-A was significantly enriched in carcinogenic activation pathways including ECM receptor interaction, TGF beta signalling pathway and cell adhesion (Fig. 5A–B). m6Acluster-B was enriched in pathways related to immune activation, such as cytokine–cytokine receptor interaction and T cell receptor signalling (Fig. 5A, C). m6Acluster-C was strongly linked to immune suppression (Fig. 5B–C). Moreover, differential expression analysis showed that m6Acluster-A exhibited increased IGFBP3 expression and decreased expression of other m^{6}A regulators; m6Acluster B was characterised by high expression of VIRMA, ZC3H13, RBM15, RBM15B, YTHDC2, YTHDF2, IGFBP1 and RBMX and m6Acluster C had significantly high expression of METTL14, YTHDC1, YTHDF1, YTHDF3, HNRNPC, HNRNPA2B1 and IGFPB2 (Fig. 4C). The m^{6}A regulators network depicted the entire landscape of interactions among the m^{6}A regulators and their prognostic significance in patients with AML (Fig. 4D). We discovered that not only did m^{6}A regulators in the same functional category show a remarkable correlation in expression, but there was also a significant correlation between writers and readers. In addition, we analysed prognostic of the three m^{6}A modification patterns and observed that the m6Acluster-A modification pattern had a clear survival advantage (Fig. 4E). From above, we considered that the composition of m^{6}A regulators may influence the formation of m^{6}A modification patterns. And distinct patten had specific biological behaviours, which were relevant to survival of AML patients.

3.5 Gene Ontology (GO) and Kyoto Encyclopedia of Genes and Genomes (KEGG) pathway enrichment analyses

We next explored the potential functions of DEGs among three m^{6}A modification patterns, 122 m^{6}A phenotype-related DEGs were identified through the limma package (Fig. 6A). GO term analysis showed that BP terms indicated that the DEGs were primarily enriched in ‘translational initiation’, CC ascribed to these DEGs mainly included ‘ribosomal subunit’ and ‘cytosolic small ribosomal subunit’ and the primary MFs included ‘structural constituent of ribosome’. The KEGG pathway enrichment analysis revealed that the DEGs were mainly enriched in pathways related to ‘fatty acid metabolism’, ‘ribosome’ and ‘fatty acid biosynthesis’.

3.6 m6Ascore is associated with the overall survival of AML patients

Among above DEGs, we identified 28 prognosis-related DEGs (Table S2). Based on them, we constructed a m6Ascore system to better illustrate the characteristics of m6A signature. We classified 145 AML patients into high- (n = 120) and low-m6Ascore groups (n = 25). The analyses indicated that OS was significantly better in the high-m6Ascore group than in the low-m6Ascore group (Fig. 7A). Besides, there was a positive correlation between m6Ascore and TMB (Fig. 7B). Then, we further confirmed the prognostic value of TMB in AML patients and found that OS did not significantly differ between the high- and low-TMB groups (Fig. 7C). Stratified survival analyses suggested that m6Ascore might serve as a potential predictor independent of TMB for AML patients (Fig. 7D).

3.7 Characteristics of TME cell infiltration in m^6A modification of AML

The TME has a strong influence on the progression of AML. Then, we analysed the TME cell infiltration found that the three m^6A modification patterns had obviously different in TME cell infiltration characteristics (Fig. 8A). m6Acluster-A was remarkably rich in innate immune cell infiltration including B cells, $CD4^+$ T cells, CD56 bright natural killer cells and immature dendritic cells. And this m^6A modification pattern revealed a matching survival advantage (Fig. 4E). m6Acluster-B was mainly enriched in immature B cells, natural killer cells, T follicular helper cells, type 1 T helper cells, type 17 T helper cells and type 2 T helper cells, whereas m6Acluster-C was characterised by immune suppression. To better understand the characteristics of TME cell infiltration, we examined the correlation between infiltrating immune cells and m6Ascore (Fig. 8B). The results showed that m6Ascore had a strong correlation with various immune cells. Moreover, there was a close relationship among various immune cells. We specifically collected PBMCs of AML patients to detect $CD4^+$T, $CD8^+$T cells, B cells and $CD56^+$ NK cells. Compared with normal samples, AML patients had an increased number of those cells (Fig. 8C). The above findings demonstrated that m^6A modification act a vital role in regulation of tumor microenvironment. And also indicated us that m^6A modification patterns and m6Ascore may be used to evaluate the tumor microenvironment features in AML.

3.8 Experimental verification of the mRNA and protein levels of m^6A regulators

In order to confirm the expression of YTHDC2, METTL14, RBM15 and ZC3H13, the total RNA of AML samples was isolated for qRT-PCR (Fig. 9). These genes were differentially expressed in normal and AML samples. Additionally, two genes were verified at the protein level, RBM15 was upregulated and METTL14 was downregulated in patients with AML, which was consistent with the results of qRT-PCR. These genes were verified successfully and showed good correspondence with the results of transcriptomic analysis, which yielded precise and reliable microarray results.

3.9 Validation in the GEO database

Based on GSE23312 datasets, we further verified the prognostic values of YTHDC2, METTL14, RBM15 and ZC3H13. Consistent with the above findings, YTHDC2 and METTL14 were positively associated with overall survival; but RBM15 and ZC3H13 were related to a poor prognosis in AML (Fig. 10).

4. Discussion

AML is a heterogeneous malignant clonal disease that prevents normal myeloid differentiation [1]. Although remission is achieved via chemotherapy in many patients, relapse is common and leads to treatment failure. In eukaryotes, m^6A is the most common form of mRNA modification [30]. Increasing evidence demonstrates that m^6A modification and its regulatory proteins play an essential role in various cancers, including leukemia [14, 31], brain tumor [32], breast cancer [33] and lung cancer [34]. Differential expression of specific RNA m^6A regulators is associated with dysregulated RNAs in tumors, and the same m^6A regulators may have varying functions in different tumors [35]. Integrating and reanalysing genomic profiles of m^6A regulators from public databases may enhance our understanding of the potential role of m^6A regulators in AML and provide more effective treatment strategies.

In this study, we examined the role of m^6A regulators in the prognosis of AML. First, we noted that METTL14, YTHDC2, ZC3H13, RBM15 and LRPPRC were significantly differentially expressed in AML patients and normal samples. Among them, METTL14, YTHDC2, ZC3H13 and RBM15 were associated with the OS of AML. The mRNA expression of METTL14, YTHDC2, ZC3H13 and RBM15 and the protein expression of METTL14 and RBM15 were successfully verified in clinical samples. METTL14 is involved in the formation of the methyltransferase complex and acts as an RNA-binding platform to form a stable heterodimer with METTL3 [36, 37]. Moreover, METTL14 mediates erythropoiesis by promoting the translation of related genes [38]. Studies showed that METTL14 acts as a tumor suppressor gene in hepatocellular carcinoma (HCC) [39] and colorectal cancer (CRC) [40]. Weng H et al. [15] reported that METTL14 promotes AML development as well as the maintenance and self-renewal of leukemia stem/initiation cells. YTHDC2 is important for increasing the translation efficiency of mRNAs [41, 42]. Yang Li et al. [43] found that YTHDC2 is a tumor suppressor gene and is correlated with immune infiltration, which may become a potential marker for head and neck squamous cell carcinoma (HNSCC) prognosis and immune infiltration. We found that the mRNA lever of YTHDC2 was reduced in AML patients. Therefore, we speculated that YTHDC2 may play a similar role in AML. Furthermore, RBM15 and its paralogue, RBM15B [44], and ZC3H13 [45] are the components of the m^6A methyltransferase complex and required for m^6A methylation. RBM15/RBM15B plays a critical role in X-inactivation and gene silencing by mediating m^6A methylation of the lncRNA XIST [44]. ZC3H13 induces the nuclear localisation of the ZC3H13–WTAP–Virilizer–Hakai complex, which regulates m^6A methylation and the self-renewal of embryonic stem cells [45]. It has been reported that METTL14 and ZC3H13 act as tumor suppressor genes and predict poor prognosis in breast cancer [46]. However, their regulatory mechanisms in AML remain uncertain.

Previous studies have indicated that AML is highly dependent on the bone marrow (BM) microenvironment that influences the survival, the proliferation and therapeutic resistance of AML cells [47, 48]. In this study, we determined three m^6A methylation modification patterns based on 22 m^6A regulators in AML patients. These three patterns showed markedly distinct TME cell infiltration characteristics. m6Acluster-C was characterised by immune suppression, and survival analysis showed that this m^6A modification pattern had the worst survival outcome. Differential expression analysis revealed that many m^6A regulators were differently expressed in the three groups. Therefore, m^6A regulators may play an indispensable role in the formation of a complex BM microenvironment.

We further identified common DEGs in the three groups. GO analysis found that these DEGs were mainly enriched in pathways related to translational initiation (BPs), ribosomal subunit and cytosolic small ribosomal subunit (CCs) and structural constituent of ribosome (MFs). Moreover, according to KEGG pathway enrichment analysis, the DEGs were mainly enriched in pathways correlated with fatty acid metabolism, ribosome metabolism and fatty acid biosynthesis. These results suggested that m^6A regulators are closely related to metabolism. Accumulating evidence suggests that m^6A RNA methylation greatly impacts RNA metabolism [49]. With regarded to molecular mechanisms, m^6A methylation affects almost every aspect of RNA metabolism, including mRNA translation, degradation, splicing, export and folding [50, 51].

In conclusion, we comprehensively investigated the landscape characteristics of m^6A regulators in AML. METTL14, YTHDC2, ZC3H13 and RBM15 were significantly correlated with OS. And they were differentially expressed between AML and normal samples. This study emphasised the role of m^6A regulators in the progression of AML and identified potential prognostic indicators for AML. In addition, the comprehensive evaluation of m^6A modification patterns may improve our understanding of the characteristics of immune cell infiltration in the TME and guide more effective immunotherapy strategies. In brief, this study provides novel insights into the potential role of m^6A regulators in AML progression and highlights the prospective use of m^6A regulators as diagnostic biomarkers and therapeutic targets for AML.

Declarations

Acknowledgements

We gratefully acknowledge the TCGA and GEO databases for the available data. And thank the National Key Clinical Specialty Discipline Construction Program and Clinical Research Center for hematological malignancies of Fujian province.

Author contributions

Xinai Liao: Methodology, data curation, original draft preparation. **Ling Chen:** Methodology, visualization. **Jingru Liu:** Methodology, investigation. **Haoran Hu:** investigation, software. **Diyu**

Hou: Methodology, validation. **Ruolan You:** Methodology, software. **Xiaoting Wang:** Methodology, investigation. **Huifang Huang**: Conceptualization, supervision and reviewing and editing. All authors read and approved the final manuscript.

Funding

This work was supported by grants from the National Natural Science Foundation of China (82070145, 81902125), Joint Funds for the Innovation of Science and Technology in Fujian Province (2019Y9073), Fujian Province Natural Science Foundation (2020J01991), the Government-funded Project of the Construction of High-level Laboratory and the Construction Project of Fujian Medical Center of Hematology (Min201704).

Availability of data and materials

All data used in the study will be shared on reasonable request to the corresponding author.

Ethics approval and consent to participate

All experimental protocols in this study were approved by Committee for the Ethical Review of Research, Fujian Medical University Union Hospital and informed consent was obtained from all the patients.

Consent for publication

Not applicable.

Competing interests

All authors declare that they have no conflicts of interest to this work.

References

1. Hu L, Gao Y, Shi Z, Liu Y, Zhao J, Xiao Z, Lou J, Xu Q, Tong X. DNA methylation-based prognostic biomarkers of acute myeloid leukemia patients. Ann Transl Med. 2019;7:737.
2. Siegel RL, Miller KD, Jemal A. Cancer statistics, 2020. CA Cancer J Clin. 2020;70:7–30.
3. Yan H, Qu J, Cao W, Liu Y, Zheng G, Zhang E, Cai Z. Identification of prognostic genes in the acute myeloid leukemia immune microenvironment based on TCGA data analysis. Cancer Immunol Immunother. 2019;68:1971–8.
4. Ferrara F, Palmieri S, Leoni F. Clinically useful prognostic factors in acute myeloid leukemia. Crit Rev Oncol Hematol. 2008;66:181–93.
5. Liu N, Pan T. RNA epigenetics. Transl Res. 2015;165:28–35.
6. Li S, Mason CE. The pivotal regulatory landscape of RNA modifications. Annu Rev Genomics Hum Genet. 2014;15:127–50.

7. Desrosiers R, Friderici K, Rottman F. Identification of methylated nucleosides in messenger RNA from Novikoff hepatoma cells. Proc Natl Acad Sci U S A. 1974;71:3971–5.
8. Niu Y, Zhao X, Wu YS, Li MM, Wang XJ, Yang YG. N6-methyl-adenosine (m6A) in RNA: an old modification with a novel epigenetic function. Genomics Proteom Bioinf. 2013;11:8–17.
9. Mill CP, Fiskus W, DiNardo CD, Qian Y, Raina K, Rajapakshe K, Perera D, Coarfa C, Kadia TM, Khoury JD, et al. RUNX1-targeted therapy for AML expressing somatic or germline mutation in RUNX1. Blood. 2019;134:59–73.
10. Hunter AM, Sallman DA. Current status and new treatment approaches in TP53 mutated AML. Best Pract Res Clin Haematol. 2019;32:134–44.
11. Monma F, Nishii K, Shiga J, Sugahara H, Lorenzo Ft, Watanabe Y, Kawakami K, Hosokai N, Yamamori S, Katayama N, Shiku H. Detection of the CBFB/MYH11 fusion gene in de novo acute myeloid leukemia (AML): a single-institution study of 224 Japanese AML patients. Leuk Res. 2007;31:471–6.
12. Mohamed AM, Balsat M, Koering C, Maucort-Boulch D, Boissel N, Payen-Gay L, Cheok M, Mortada H, Auboeuf D, Pinatel C, et al. TET2 exon 2 skipping is an independent favorable prognostic factor for cytogenetically normal acute myelogenous leukemia (AML): TET2 exon 2 skipping in AML. Leuk Res. 2017;56:21–8.
13. Spencer DH, Russler-Germain DA, Ketkar S, Helton NM, Lamprecht TL, Fulton RS, Fronick CC, O'Laughlin M, Heath SE, Shinawi M, et al. CpG Island Hypermethylation Mediated by DNMT3A Is a Consequence of AML Progression. Cell. 2017;168:801–16.e813.
14. Li Z, Weng H, Su R, Weng X, Zuo Z, Li C, Huang H, Nachtergaele S, Dong L, Hu C, et al. FTO Plays an Oncogenic Role in Acute Myeloid Leukemia as a N(6)-Methyladenosine RNA Demethylase. Cancer Cell. 2017;31:127–41.
15. Weng H, Huang H, Wu H, Qin X, Zhao BS, Dong L, Shi H, Skibbe J, Shen C, Hu C, et al. METTL14 Inhibits Hematopoietic Stem/Progenitor Differentiation and Promotes Leukemogenesis via mRNA m(6)A Modification. Cell Stem Cell. 2018;22:191–205.e199.
16. Wang X, Lu Z, Gomez A, Hon GC, Yue Y, Han D, Fu Y, Parisien M, Dai Q, Jia G, et al. N6-methyladenosine-dependent regulation of messenger RNA stability. Nature. 2014;505:117–20.
17. Colaprico A, Silva TC, Olsen C, Garofano L, Cava C, Garolini D, Sabedot TS, Malta TM, Pagnotta SM, Castiglioni I, et al. TCGAbiolinks: an R/Bioconductor package for integrative analysis of TCGA data. Nucleic Acids Res. 2016;44:e71.
18. Ritchie ME, Phipson B, Wu D, Hu Y, Law CW, Shi W, Smyth GK. limma powers differential expression analyses for RNA-sequencing and microarray studies. Nucleic Acids Res. 2015;43:e47.
19. de Hoon MJ, Imoto S, Nolan J, Miyano S. Open source clustering software. Bioinformatics. 2004;20:1453–4.
20. Mayakonda A, Lin DC, Assenov Y, Plass C, Koeffler HP. Maftools: efficient and comprehensive analysis of somatic variants in cancer. Genome Res. 2018;28:1747–56.
21. Wilkerson MD, Hayes DN. ConsensusClusterPlus: a class discovery tool with confidence assessments and item tracking. Bioinformatics. 2010;26:1572–3.

22. Symsack A, Gaunaurd I, Thaper A, Springer B, Bennett C, Clemens S, Lucarevic J, Kristal A, Sumner M, Isaacson B, et al. Usability Assessment of the Rehabilitation Lower-limb Orthopedic Assistive Device by Service Members and Veterans With Lower Limb Loss. Mil Med. 2021;186:379–86.
23. Hanzelmann S, Castelo R, Guinney J. GSVA: gene set variation analysis for microarray and RNA-seq data. BMC Bioinformatics. 2013;14:7.
24. Zeng L, Fan X, Wang X, Deng H, Zhang K, Zhang X, He S, Li N, Han Q, Liu Z. Bioinformatics Analysis based on Multiple Databases Identifies Hub Genes Associated with Hepatocellular Carcinoma. Curr Genomics. 2019;20:349–61.
25. Yu G, Wang LG, Han Y, He QY. clusterProfiler: an R package for comparing biological themes among gene clusters. Omics. 2012;16:284–7.
26. Zeng D, Li M, Zhou R, Zhang J, Sun H, Shi M, Bin J, Liao Y, Rao J, Liao W. Tumor Microenvironment Characterization in Gastric Cancer Identifies Prognostic and Immunotherapeutically Relevant Gene Signatures. Cancer Immunol Res. 2019;7:737–50.
27. Charoentong P, Finotello F, Angelova M, Mayer C, Efremova M, Rieder D, Hackl H, Trajanoski Z. Pan-cancer Immunogenomic Analyses Reveal Genotype-Immunophenotype Relationships and Predictors of Response to Checkpoint Blockade. Cell Rep. 2017;18:248–62.
28. Barbie DA, Tamayo P, Boehm JS, Kim SY, Moody SE, Dunn IF, Schinzel AC, Sandy P, Meylan E, Scholl C, et al. Systematic RNA interference reveals that oncogenic KRAS-driven cancers require TBK1. Nature. 2009;462:108–12.
29. Quintás-Cardama A, Hu C, Qutub A, Qiu YH, Zhang X, Post SM, Zhang N, Coombes K, Kornblau SM. p53 pathway dysfunction is highly prevalent in acute myeloid leukemia independent of TP53 mutational status. Leukemia. 2017;31:1296–305.
30. Liu N, Pan T. N6-methyladenosine–encoded epitranscriptomics. Nat Struct Mol Biol. 2016;23:98–102.
31. Bansal H, Yihua Q, Iyer SP, Ganapathy S, Proia DA, Penalva LO, Uren PJ, Suresh U, Carew JS, Karnad AB, et al. WTAP is a novel oncogenic protein in acute myeloid leukemia. Leukemia. 2014;28:1171–4.
32. Zhang S, Zhao BS, Zhou A, Lin K, Zheng S, Lu Z, Chen Y, Sulman EP, Xie K, Bögler O, et al. m(6)A Demethylase ALKBH5 Maintains Tumorigenicity of Glioblastoma Stem-like Cells by Sustaining FOXM1 Expression and Cell Proliferation Program. Cancer Cell. 2017;31:591–606.e596.
33. Zhang C, Samanta D, Lu H, Bullen JW, Zhang H, Chen I, He X, Semenza GL. Hypoxia induces the breast cancer stem cell phenotype by HIF-dependent and ALKBH5-mediated m^6A-demethylation of NANOG mRNA. Proc Natl Acad Sci U S A. 2016;113:E2047–56.
34. Lin S, Choe J, Du P, Triboulet R, Gregory RI. The m(6)A Methyltransferase METTL3 Promotes Translation in Human Cancer Cells. Mol Cell. 2016;62:335–45.
35. Deng X, Su R, Feng X, Wei M, Chen J. Role of N(6)-methyladenosine modification in cancer. Curr Opin Genet Dev. 2018;48:1–7.

36. Wang X, Feng J, Xue Y, Guan Z, Zhang D, Liu Z, Gong Z, Wang Q, Huang J, Tang C, et al. Structural basis of N(6)-adenosine methylation by the METTL3-METTL14 complex. Nature. 2016;534:575–8.
37. Liu J, Yue Y, Han D, Wang X, Fu Y, Zhang L, Jia G, Yu M, Lu Z, Deng X, et al. A METTL3-METTL14 complex mediates mammalian nuclear RNA N6-adenosine methylation. Nat Chem Biol. 2014;10:93–5.
38. Kuppers DA, Arora S, Lim Y, Lim AR, Carter LM, Corrin PD, Plaisier CL, Basom R, Delrow JJ, Wang S, et al. N(6)-methyladenosine mRNA marking promotes selective translation of regulons required for human erythropoiesis. Nat Commun. 2019;10:4596.
39. Ma JZ, Yang F, Zhou CC, Liu F, Yuan JH, Wang F, Wang TT, Xu QG, Zhou WP, Sun SH. METTL14 suppresses the metastatic potential of hepatocellular carcinoma by modulating N(6) -methyladenosine-dependent primary MicroRNA processing. Hepatology. 2017;65:529–43.
40. Yang X, Zhang S, He C, Xue P, Zhang L, He Z, Zang L, Feng B, Sun J, Zheng M. METTL14 suppresses proliferation and metastasis of colorectal cancer by down-regulating oncogenic long non-coding RNA XIST. Mol Cancer. 2020;19:46.
41. Hsu PJ, Zhu Y, Ma H, Guo Y, Shi X, Liu Y, Qi M, Lu Z, Shi H, Wang J, et al. Ythdc2 is an N(6)-methyladenosine binding protein that regulates mammalian spermatogenesis. Cell Res. 2017;27:1115–27.
42. Mao Y, Dong L, Liu XM, Guo J, Ma H, Shen B, Qian SB. m(6)A in mRNA coding regions promotes translation via the RNA helicase-containing YTHDC2. Nat Commun. 2019;10:5332.
43. Li Y, Zheng JN, Wang EH, Gong CJ, Lan KF, Ding X. The m6A reader protein YTHDC2 is a potential biomarker and associated with immune infiltration in head and neck squamous cell carcinoma. PeerJ. 2020;8:e10385.
44. Patil DP, Chen CK, Pickering BF, Chow A, Jackson C, Guttman M, Jaffrey SR. m(6)A RNA methylation promotes XIST-mediated transcriptional repression. Nature. 2016;537:369–73.
45. Wen J, Lv R, Ma H, Shen H, He C, Wang J, Jiao F, Liu H, Yang P, Tan L, et al. Zc3h13 Regulates Nuclear RNA m(6)A Methylation and Mouse Embryonic Stem Cell Self-Renewal. Mol Cell. 2018;69:1028–38.e1026.
46. Gong PJ, Shao YC, Yang Y, Song WJ, He X, Zeng YF, Huang SR, Wei L, Zhang JW. Analysis of N6-Methyladenosine Methyltransferase Reveals METTL14 and ZC3H13 as Tumor Suppressor Genes in Breast Cancer. Front Oncol. 2020;10:578963.
47. Abdul-Aziz AM, Sun Y, Hellmich C, Marlein CR, Mistry J, Forde E, Piddock RE, Shafat MS, Morfakis A, Mehta T, et al. Acute myeloid leukemia induces protumoral p16INK4a-driven senescence in the bone marrow microenvironment. Blood. 2019;133:446–56.
48. Tabe Y, Konopleva M. Role of Microenvironment in Resistance to Therapy in AML. Curr Hematol Malig Rep. 2015;10:96–103.
49. Wang T, Kong S, Tao M, Ju S. The potential role of RNA N6-methyladenosine in Cancer progression. Mol Cancer. 2020;19:88.

50. Liu Q, Gregory RI. RNAmod: an integrated system for the annotation of mRNA modifications. Nucleic Acids Res. 2019;47:W548-w555.
51. Liu N, Zhou KI, Parisien M, Dai Q, Diatchenko L, Pan T. N6-methyladenosine alters RNA structure to regulate binding of a low-complexity protein. Nucleic Acids Res. 2017;45:6051–63.

Tables

Table 1. Details on AML patient samples

NO.	Gender	Age	WBC(10^9/L)	FAB	Mutation Status
AML#1	Female	44	1	M0	None
AML#2	Male	62	15.45	M5	CBL;KIT
AML#3	Male	43	4.08	M2	None
AML#4	Male	39	2.8	M5	PTPN11
AML#5	Female	47	6.59	M5	CEBPA
AML#6	Male	45	25.79	M5	TP53;TET2;CEBPA
AML#7	Male	54	1	M5	WT1
AML#8	Male	68	0.76	M2	None
AML#9	Male	34	38.12	M5	NPM1;NRAS;FLT3-TKD
AML#10	Female	67	1.16	M5	DNMT3A;NPM1;PTPN11
AML#11	Male	59	3.18	M2	FLT3-ITD;NPM1;IDH2
AML#12	Male	34	67.5	M5	CBFb-MYH11
AML#13	Male	56	1.81	M5	None
AML#14	Female	54	1.97	M5	BCR/ABL1
AML#15	Male	14	92.5	M5	FLT3-TKD;RUNX1;PTPN11;PHF6

Figures

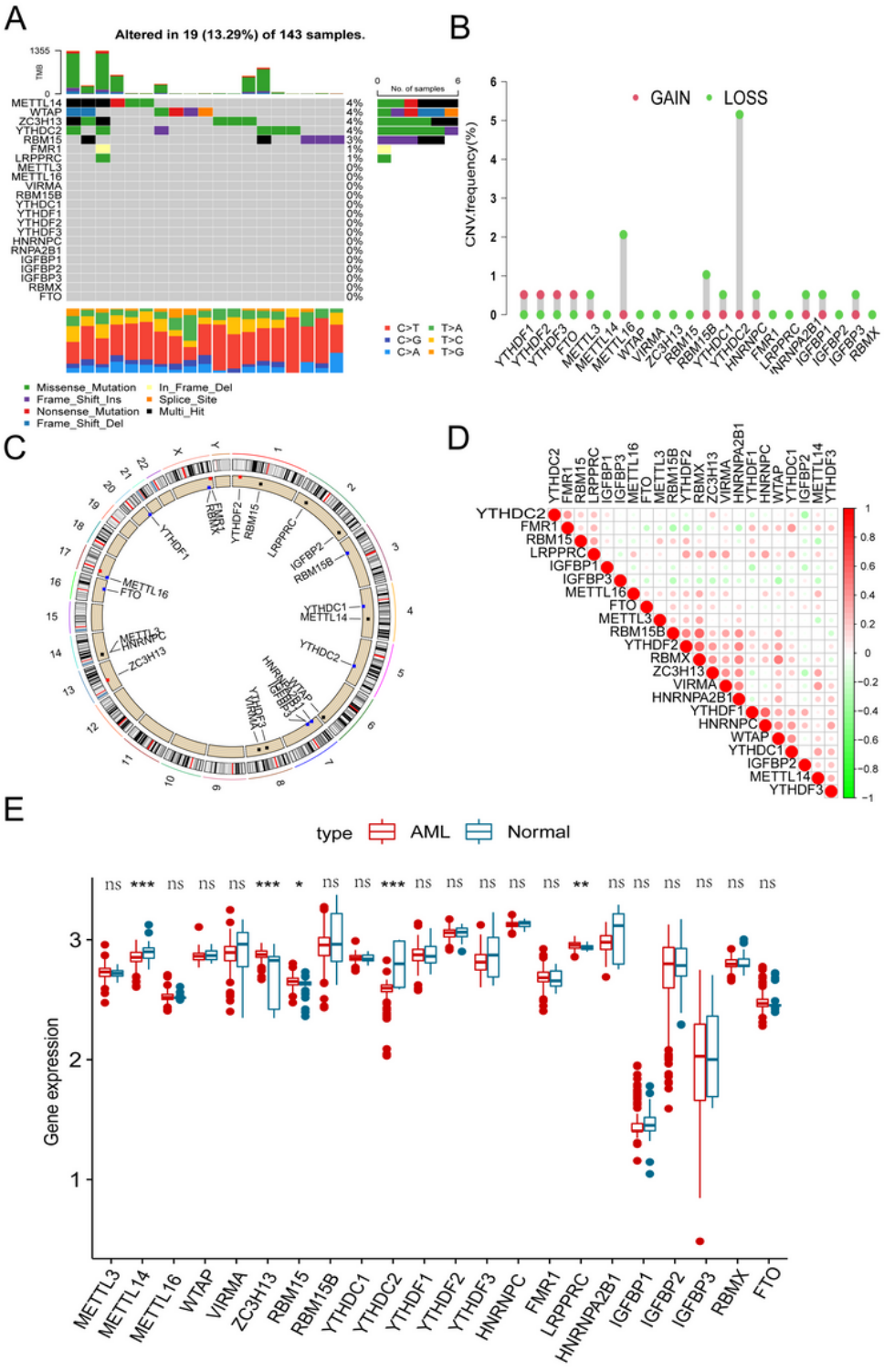

Figure 1

Genetic variation landscape and expression of m^{6}A regulators in AML patients. (A) The frequency of mutations in 22 m^{6}A regulators in 143 AML samples obtained from TCGA database. (B) The frequency of CNVs in m^{6}A regulators in TCGA cohort. (C) The location of CNVs in m^{6}A regulators on 22 chromosomes

in TCGA cohort. (D) Co-expression of m^6A regulators analysed and visualised via Pearson correlation analysis. (E) Comparison of the expression of 22 m^6A regulators in normal and AML samples

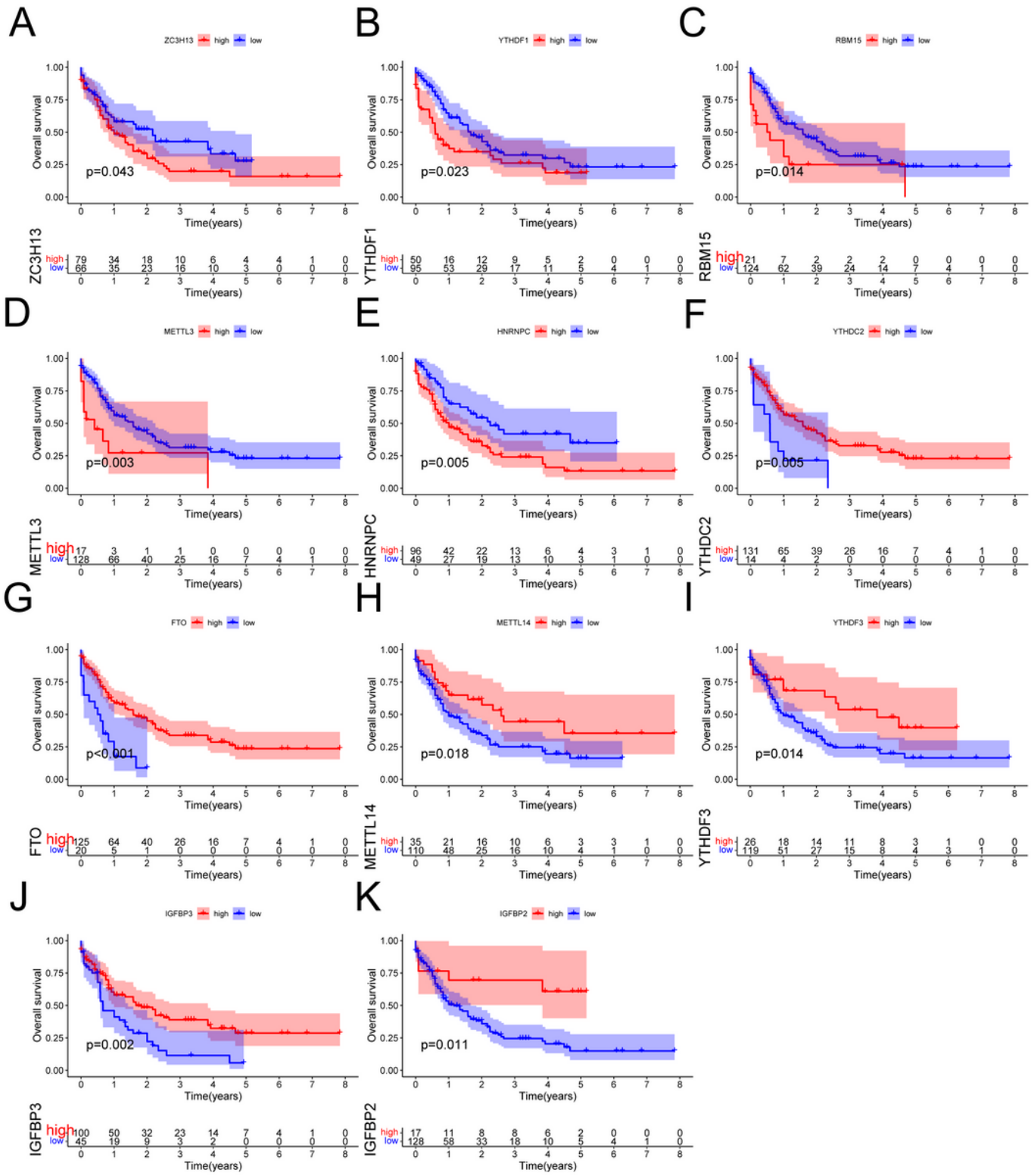

Figure 2

Overall survival analysis of m^{6}A regulators. (A–K) Survival curve analysis of m^{6}A regulators, which were significantly related to the prognosis of AML in TCGA database. TCGA, The Cancer Genome Atlas

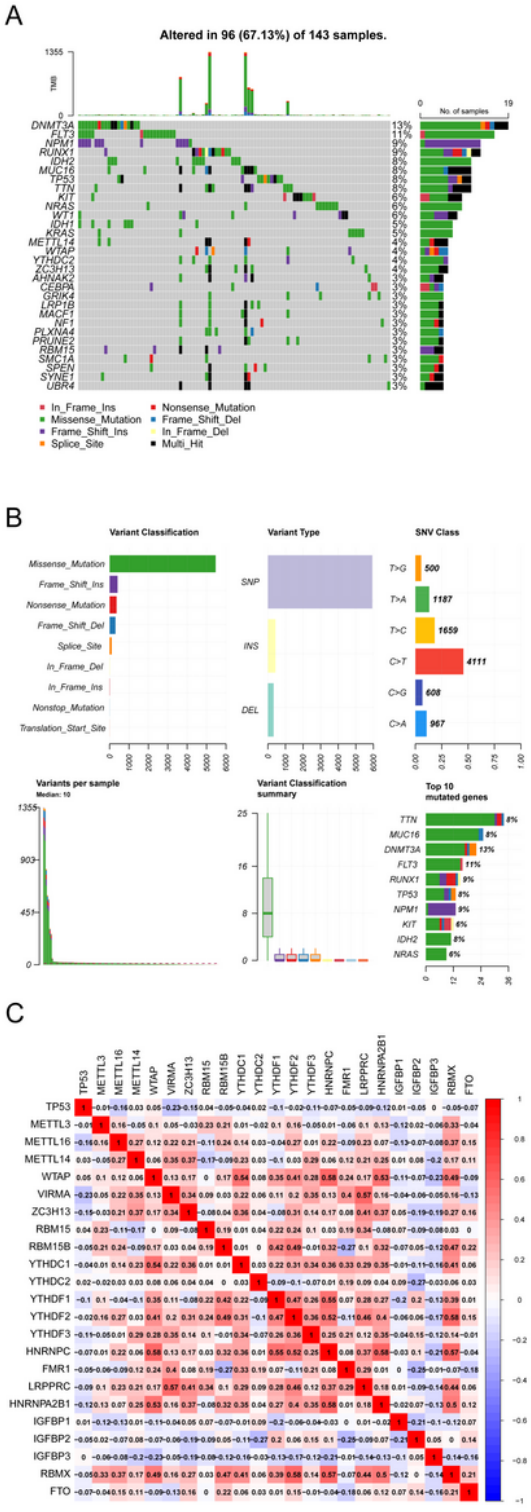

Figure 3

Analyses of somatic mutation profiles in AML samples. (A) The waterfall plot demonstrating extensive mutation information for the top 30 genes of each sample, with distinct colour annotations to classify different mutation types. (B) According to several classification categories, missense mutations, SNPs and C > T mutations accounted for the vast majority of mutations. The total number of mutations is shown along with the box plots of each variant. The top 10 mutant genes in patients with AML are also shown. (C) Correlation between the expression of TP53 and m^{6}A regulators. Positive correlation is shown in red, and negative correlation is shown in blue

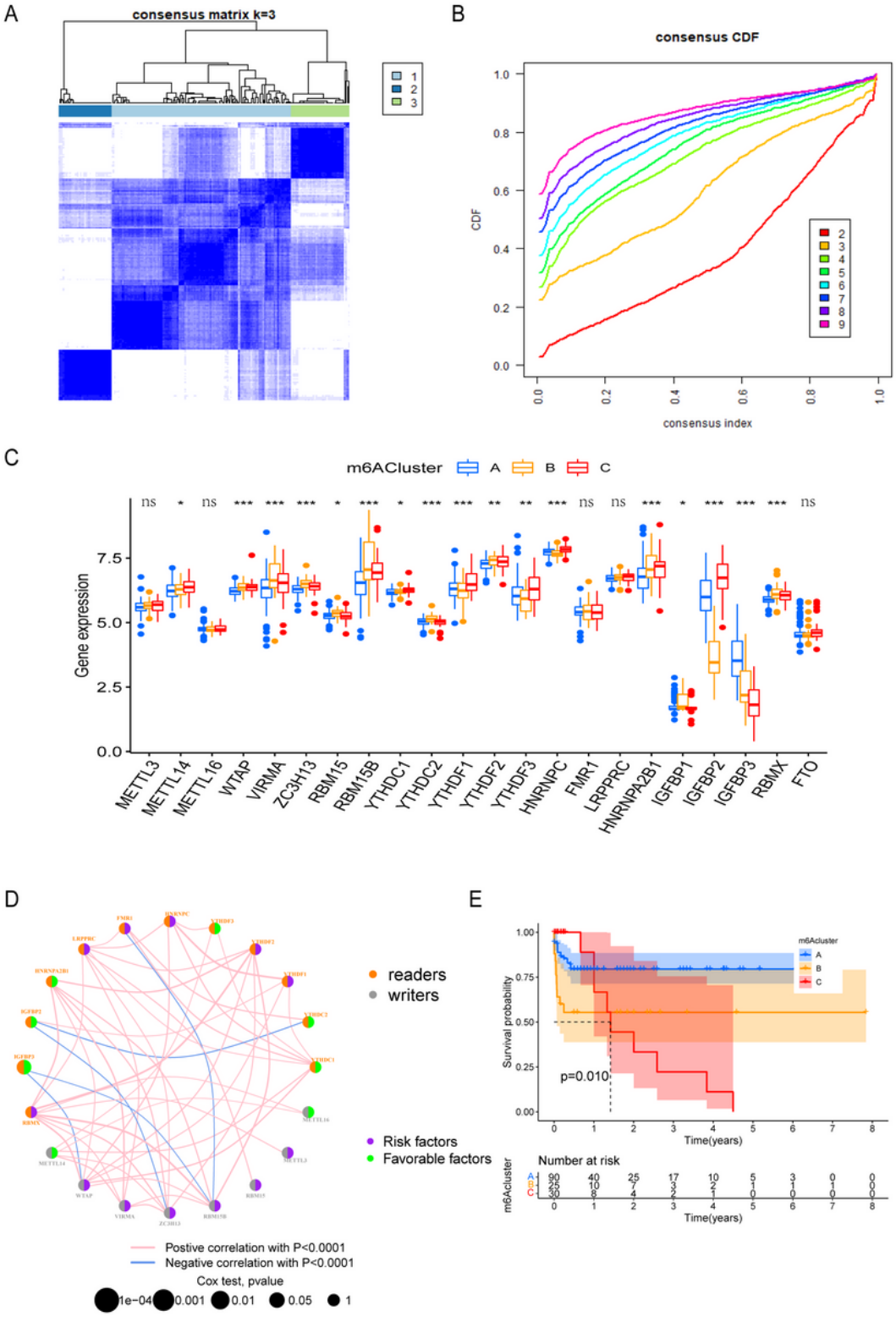

Figure 4

Patterns of m^{6}A methylation modification. (A) Consensus matrices of TCGA cohort for k = 3. (B) Consensus CDF of TCGA cohort for k = 2–9. (C) Expression of m^{6}A regulators in three m6Aclusters. (D) Interaction among m^{6}A regulators in AML. (E) Survival analyses for the three m^{6}A modification patterns

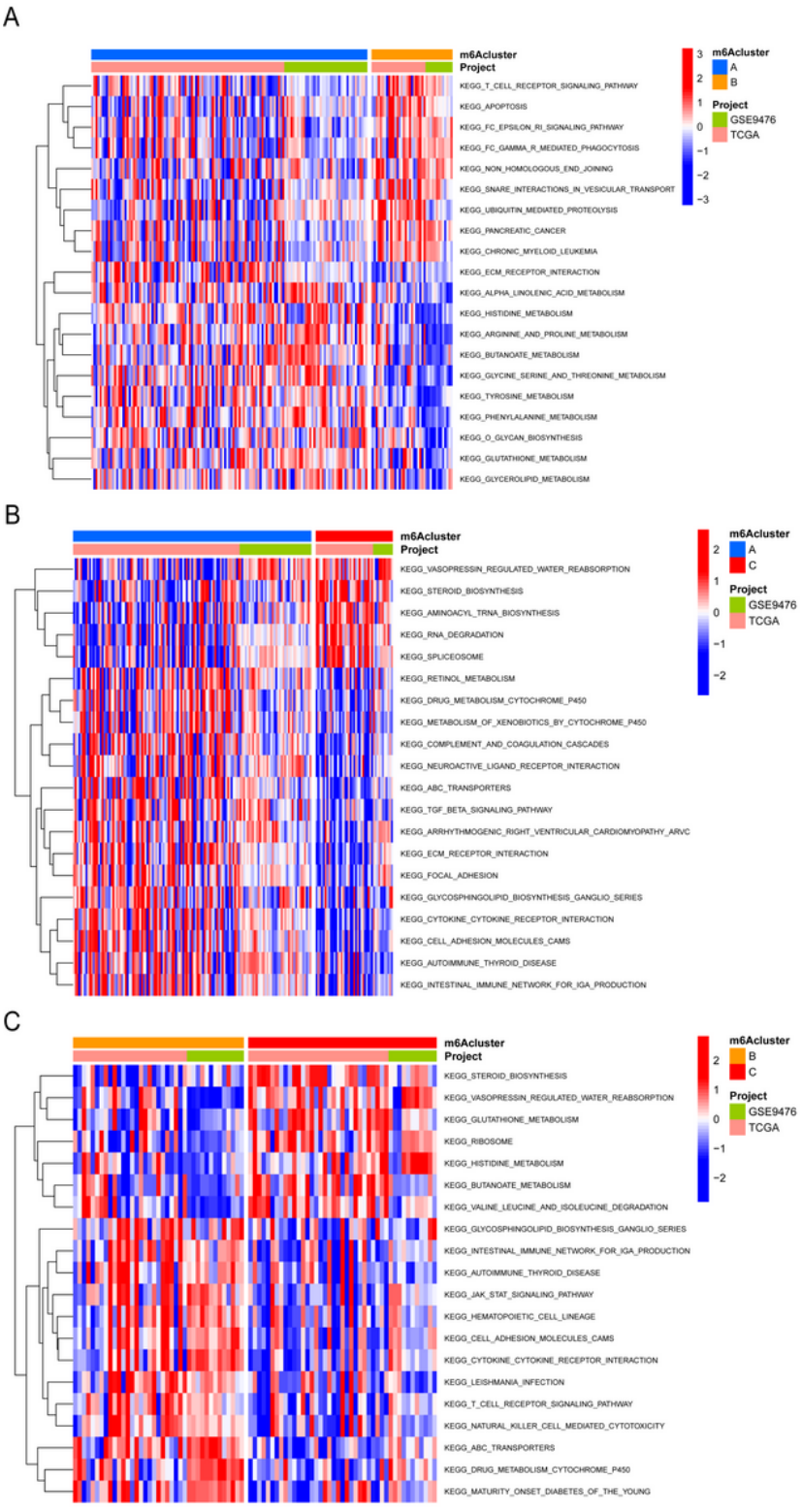

Figure 5

Biological characteristics of each modification pattern. (A–C) GSVA of distinct m^{6}A modification patterns reveals the activation states of biological pathways in each pattern. (A) m6Acluster-A versus m6Acluster-B; (B) m6Acluster-B versus m6Acluster-C; (C) m6Acluster-A versus m6Acluster-C

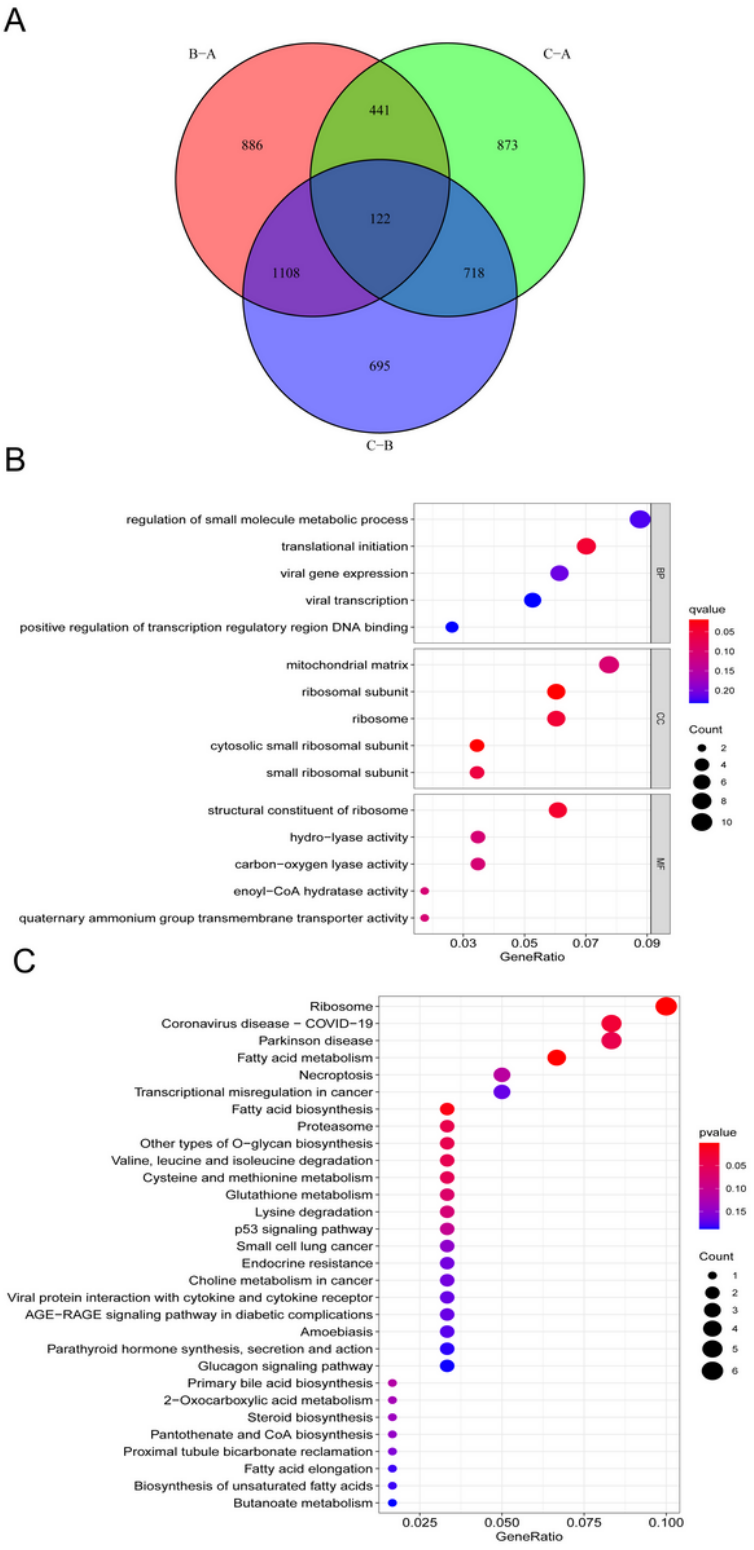

Figure 6

Functional annotation of m^{6}A-related DEGs in AML. (A) Venn diagram showing 122 m^{6}A-related DEGs identified using the limma package. (B) Functional annotation of DEGs using GO enrichment analysis. The colour depth of circles represents the q-value, and the size represents the number of genes enriched. (C) KEGG pathway analysis of DEGs. The colour depth of the circle represents the P-value, and the size represents the number of genes enriched

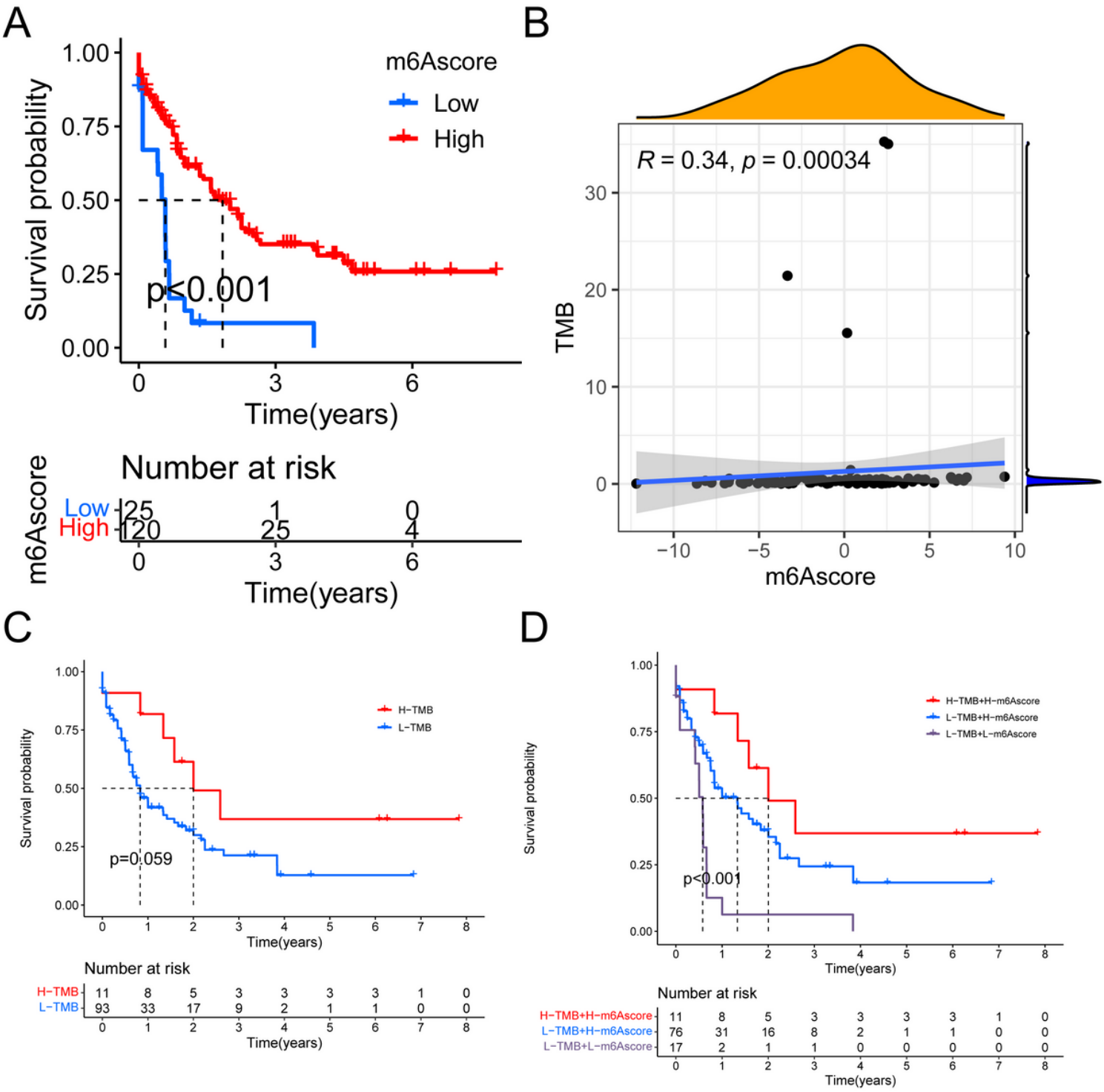

Figure 7

m6Ascore is independently associated with the overall survival of patients with AML. (A) Kaplan–Meier survival curves of the low- and high-m6Ascore groups in TCGA cohort. (B) The correlation between TMB and m6Ascore. (C) Kaplan–Meier survival curves of the low- and high-TMB groups in TCGA cohort. (D) Kaplan–Meier survival curves for subgroup patients stratified by both m6Ascore and TMB

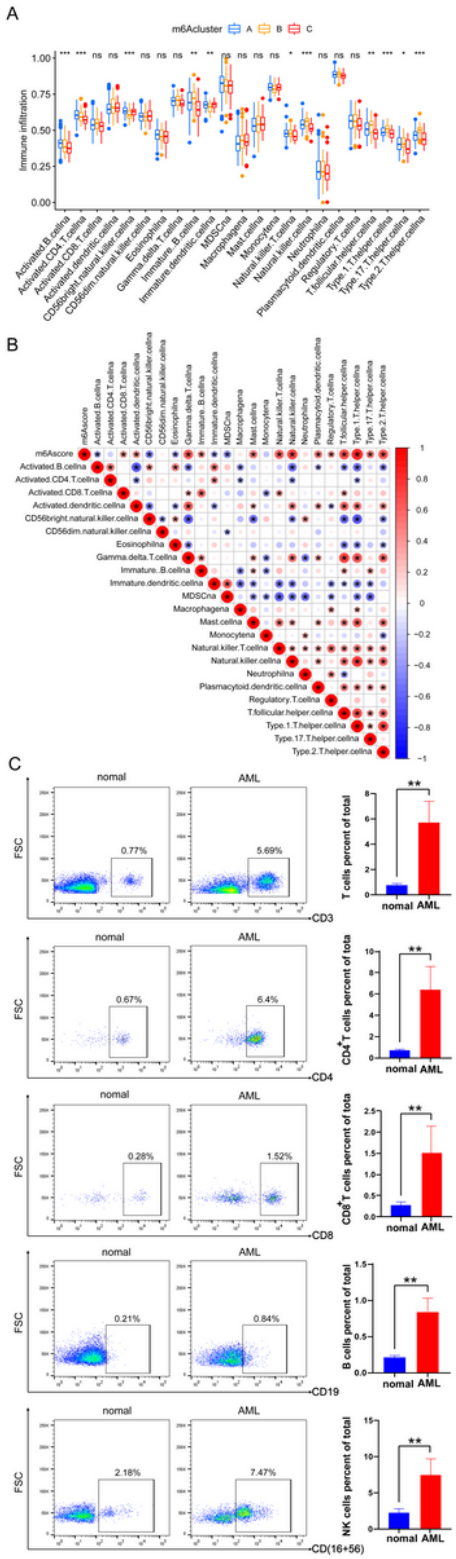

Figure 8

TME cell infiltration characteristics of patients with AML. (A) Abundance of immune-infiltrating cells in TME in the three m^{6}A modification patterns. (B) Correlation between m6Ascore and infiltrating cells in TME. (C) Flow cytometry analysis for the evaluation of the number of T cells, B cells and NK cells in normal and AML samples

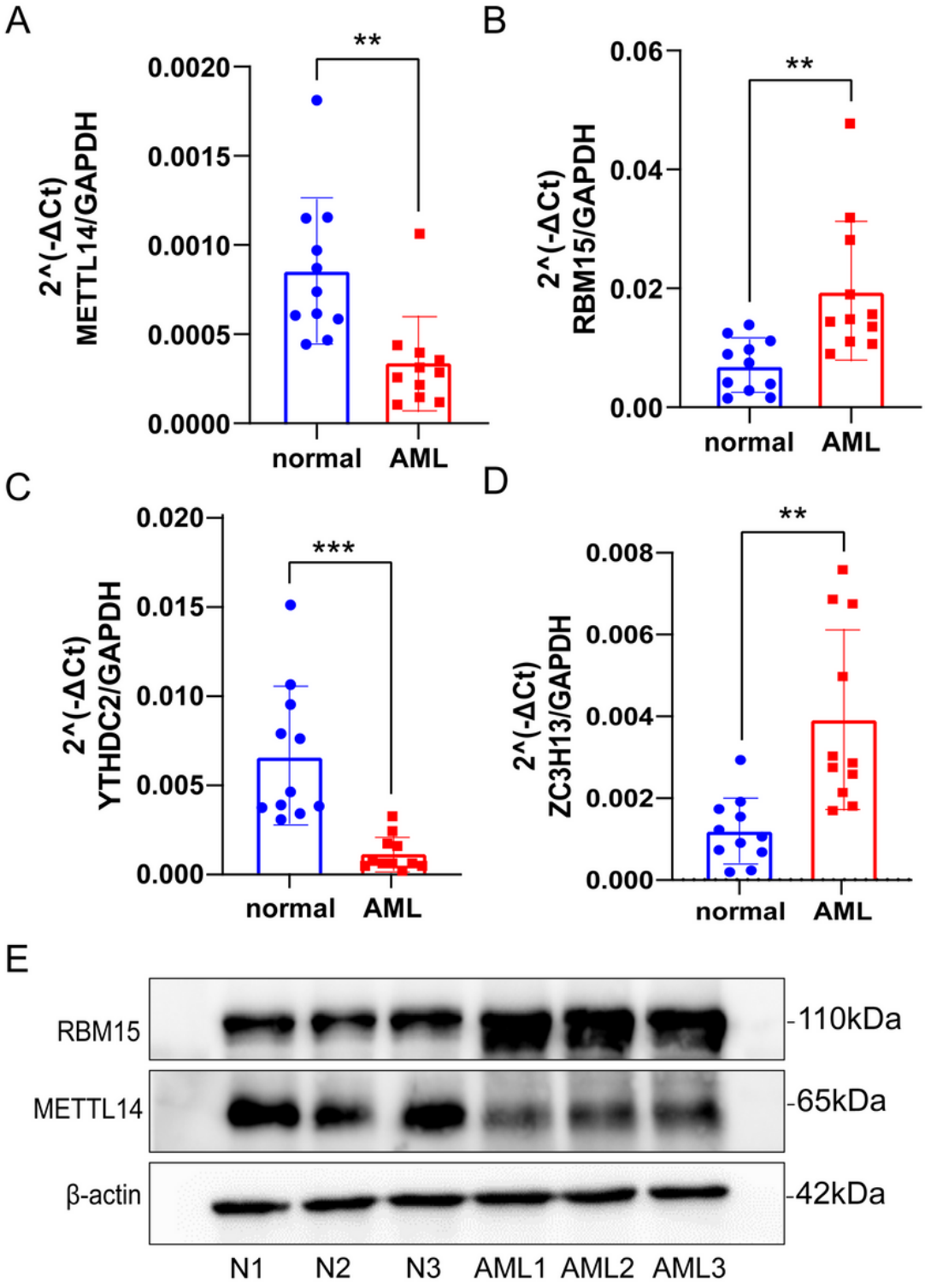

Figure 9

Validation of the expression of m^{6}A regulators via qRT-PCR and western blot. (A–D) The mRNA expression of METTL14, RBM15, YTHDC2 and ZC3H13 in AML and normal samples as determined via qRT-PCR. (E) METTL14 and RBM15 protein expression were detected in three pairs of AML and normal samples via western blotting

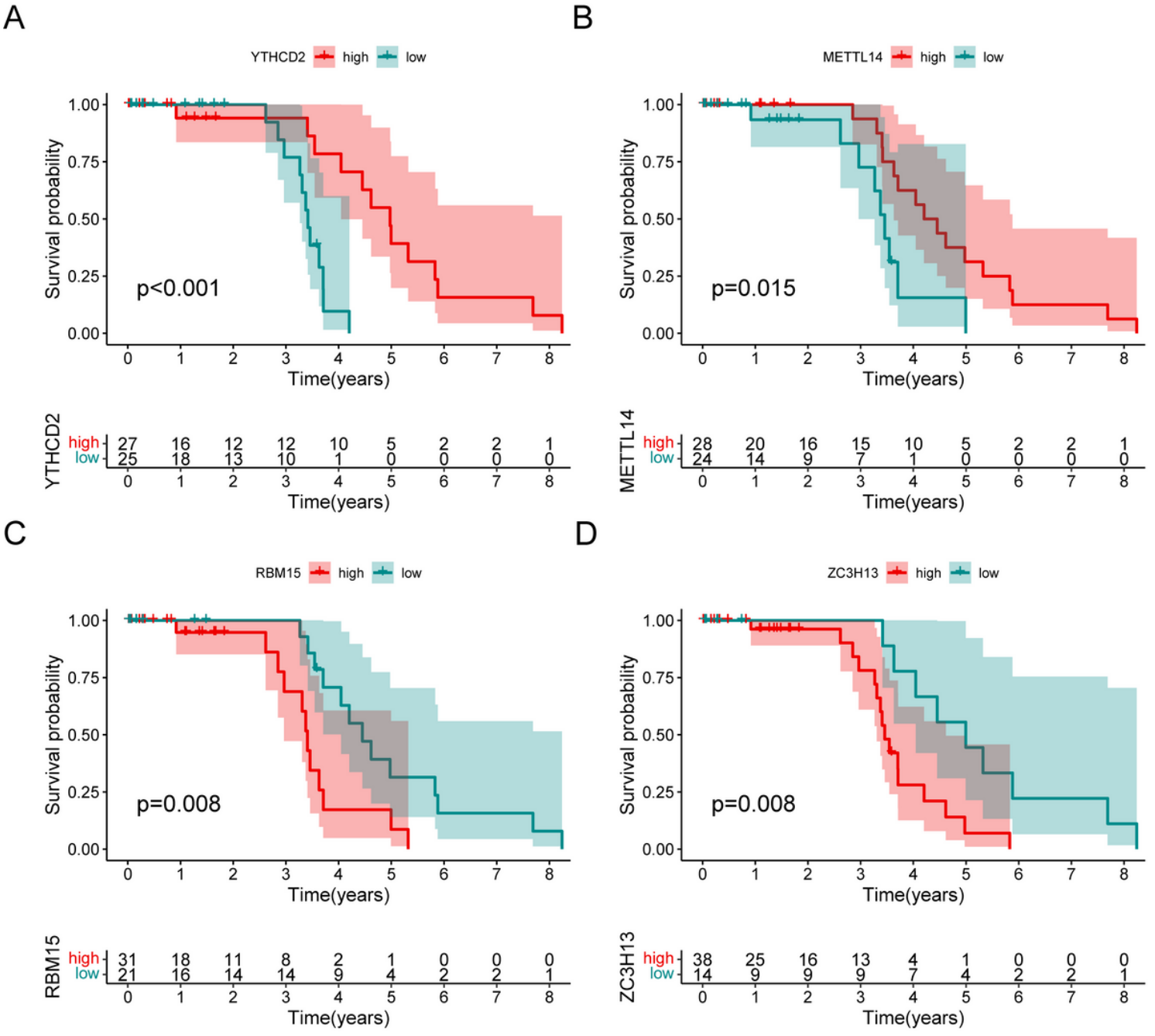

Figure 10

Verification the prognostic value of genes in the GEO database. (A-D) Survival analysis was performed for subgroups of patients stratified by YTHDC2 (A), METTL14 (B), RBM15 (C) and ZC3H13 (D) expression (*P*

< 0.05, log-rank test)

Supplementary Files

This is a list of supplementary files associated with this preprint. Click to download.

- SupplementaryTable1.xlsx
- SupplementaryTable2.xlsx
- figureS1.tif
- figureS2.tif